www.czasopisma.pan.pl PAN POLSKA AKADEMIA NAUK www.journals.pan.pl

A R C H I V E S O F M E T A L L U R G Y A N D M A T E R I A L S

Volume 57 2012 Issue 3

DOI: 10.2478/v10172-012-0076-6

K. PIEŁA*, L. BŁAŻ*, Z. SIERPIŃSKI*, T. FORYŚ*

NON-ISOTHERMAL ANNEALING OF AA7075 ALUMINUM ALLOY – STRUCTURAL AND MECHANICAL EFFECTS

NIEIZOTERMICZNE WYŻARZANIE STOPU ALUMINIUM AA7075 – EFEKTY STRUKTURALNE I MECHANICZNE

Calorimetric and dilatometric tests were performed on AA7075 aluminum alloy annealed at constant heating rate of 15°C/min in temperature range 20-470°C and discussed in relation to the hardness test and structure observation results. The samples were machined from furnace cooled material (FC), furnace cooled and deformed (FCD) material, solution treated (ST) material and solution treated and deformed (STD) material. It was found that the nucleation and growth of transition η' and stable η ($MgZn_2$) phases caused remarkable reduction of thermal expansion coefficient α_t, whereas both the dissolution of η phase and formation of GP zones were accompanied by an increase of α_t value. While η phase started to dissolve at 250°C, a widespread endothermic effect was observed on DSC curves. Dissolution of η particles at high annealing temperatures was accompanied by the solid solution hardening of the alloy. Mentioned hardening process was overlapped by expected material softening that was ascribed to recovery and recrystallization processes. Because of superposition the solution hardening and recrystallization softening, recrystallization temperature could not be precisely defined on the basis of simple hardness measurements.

Keywords: aluminum alloy, annealing, thermal treatment, structure

W pracy przedstawiono wyniki badań kalorymetrycznych, dylatometrycznych i pomiarów twardości stopu aluminium AA7075 poddanego nieizotermicznemu wyżarzaniu (nagrzewaniu ze stałą prędkością) w zakresie temperatur 20-470°C. Badania objęły cztery stany metalurgiczne materiału: wolno studzony z piecem (FC), wolno studzony z piecem i odkształcony (FCD), przesycony (ST) oraz przesycony i odkształcony (STD). Stwierdzono, że wydzielanie fazy pośredniej η' i równowagowej η($MgZn_2$) powoduje wyraźne obniżenie współczynnika rozszerzalności cieplnej α_t, natomiast zarówno rozpuszczanie fazy η, jak i formowanie stref GP prowadzi do jego wzrostu. Rozpuszczanie fazy η rozpoczyna się w temperaturze 250°C i towarzyszy mu rozległy efekt endotermiczny, a w zaawansowanym stadium rozpuszczania – także wzrost twardości przesycanych próbek, będący rezultatem umocnienia roztworowego stopu. Umocnienie roztworowe zakłóca tym samym efekt oczekiwanego mięknięcia materiału wskutek rekrystalizacji, co w konsekwencji utrudnia dokładną ocenę temperaturowego zakresu rekrystalizacji w oparciu o pomiary twardości.

1. Introduction

Structural observations by means of a common metallography method and transmission electron microscopy (TEM) including X-ray energy disperse analysis (EDX) are usually used techniques for testing phase transformations and morphology of structural components in aluminum alloys [1]. During last decades also differential scanning calorimetry (DSC) was widely accepted as the complementary method for detailed analysis of the phase transformations in the alloys. Due to the high sensitivity of modern DSC systems, very fine exo- and endothermic effects related to the specific phase transformation can be detected. In particular, combined DSC and TEM analyses supported by adequate mechanical tests were found to be very useful for tracking precipitation sequences in precipitation hardenable aluminum alloys. During heating of solution treated aluminum alloy of 7xxx series, usually two exothermic and one endothermic effects were reported. The first two peaks, denoted I and II afterwards, were ascribed to GP zones development (I) and following metastable η' and stable η($MgZn_2$) particles nucleation and growth (II). The third spread endothermic effect (III) was attributed to dissolution of η particles [1-9].

It should be stressed that the heat capacity vs. temperature curves, presented in literature for 7xxx series alloys, are not consistent and vary in the peak positioning and their intensity. These discrepancies are reported regardless of very similar composition of tested alloys and

* AGH UNIVERSITY OF SCIENCE AND TECHNOLOGY, DEPARTMENT OF STRUTURE AND MECHANICS OF SOLIDS, 30-059 KRAKOW, 30 MICKIEWICZA AV., POLAND

similar heat treatment conditions. The first exothermic peak on DSC curve, which result from GP-zones formation, is always reported for solution treated samples. However, the peak I is observed at different temperature between 75°C and 120°C [2-4]. Following peak II is also detected at different temperature, from 165-265°C to 200-300°C. The peak II is reported to appear as a single peak as well as a double – or a triple-peak that are composed of close-placed fine exothermic effects [2, 3, 5, 6]. Dissolution of particles, which result in a III-range development, usually start at 270-300°C and the most enhanced heat transfer is observed at 420-450°C, i.e. close to, or just above solvus temperature [3-7].

Precipitation hardenable aluminum alloys are often processed by means of complex thermomechanical procedures that combine both the strain hardening and ageing of the material. It is commonly believed that a solid solution decomposition and nucleation of disperse particles are affected by the dislocation substructure. Facilitated nucleation of particles on dislocation tangles is promoted due to effective core diffusion along dislocations and the privileged nucleation on structural defects. DSC analysis of solution treated and cold deformed AlZn6.1%Mg2.35% alloys revealed important effect of the preliminary deformation on the heat effects [8, 9]. Cold deformation, ε = 10%, was found to suppress the peak I and divide the peak II into three sub-peaks (150-265°C) that are ascribed to η' precipitation, transformation of η' to η and following transformation of η' into T($Al_2Zn_3Mg_3$), respectively. Position of the following peak III is reported to be practically stable with respect to preliminary heat treatment conditions. Aluminum alloys of 7xxx series often undergo highly localized deformation that result in the shear bands development. As result, the following ageing of as-deformed material results in promoted nucleation and growth of η – particles along shear bands [10, 11]. Therefore, the peak II may become broadened due to varied nucleation conditions for inhomogeneously deformed materials.

Both the phase transformation and recrystallization process are usually accompanied by the fine volume dilatability. However, the thermal expansion measurement is rarely used for the detection of some structural transformation processes in aluminum alloys [13-17]. Therefore, experiments described bellow were undertaken to study the structural transformation in solution treated AA7075 aluminum alloy including the dilatometry test at constant heating rate. Dilatometer characteristics were analyzed with respect to the hardness measurements, DSC curves, and transmission electron microscopy analysis of structural components.

2. Experimental

Experiments were performed on AA7075 aluminum alloy having a chemical composition as follows (in wt. %): Zn-5.94%, Mg-2.25%, Cu-1.46%, Fe-0.37%, Mn-0.35%, Cr-0.18%, Si-0.15%, Al – in balance. Rectangular samples, 100×10×5.8 mm in size, were cut from a hot extruded flat bar and heat treated at 465°C/1.5 h. Following furnace cooling of the samples, marked FC hereafter, was performed at constant cooling rate 20°C/h. A set of samples, marked ST (solution treated) hereafter, was cooled in cold water after the annealing. Samples denoted FCD and STD were deformed 55% using cold rolling after the heat treatment FC and ST, respectively. Tolledo's Differential Scanning Calorimeter DSC-821e and Thermomechanical Analyzer TMA/SDTA-840 were used for testing the samples at constant heating rate 15°C/min. Hardness tests were performed on samples heated up in a furnace at the same controlled heating rate 15°C/min. While designed temperature was reached, the sample was water cooled and the hardness test was performed using a Brinnell hardness tester. Structural observations were performed using a standard metallographic method and Neophot 32 microscope. However, detailed structure analysis required higher magnification. Therefore, transmission electron microscopy (TEM) observations were performed utilizing JEM 2010 TEM microscope operating at 200 kV, equipped with scanning transmission electron microscopy device (STEM) and Oxford PENTAFET energy dispersive X-ray analysis system (EDX). Thin foils for TEM observations were prepared using mechanical grinding and final thinning with Gatan PIPS 691 ion thinning machine.

3. Results and analysis

3.1. Furnace cooled specimens

Slow furnace cooling of FC-type samples result in the precipitation of constituent phases and receiving thermodynamically stabilized structure of the material. Therefore, any ageing effects can be observed during following heating of the both FC and FCD samples and received calorimetric curves become flat within temperature range 20-250°C as shown in Fig. 1a. Large endothermic effect, generally ascribed to η-particles dissolution, was observed at higher temperature range with the maximum at ~425°C. Mentioned endothermic effect was superimposed with a small exothermic peak ranging from 350°C to 410°C (maximum at ~385°C) for FCD-sample that result from recrystallization of as deformed material. Recrystallization of the mate-

rial was possible due to η-particles dissolution that released the grain boundaries and enabled their migration. The growth of as-recrystallized grains in preliminarily fibrous-like structure of the hot extruded and cold rolled material is confirmed by structural observations presented in Fig. 3a-c.

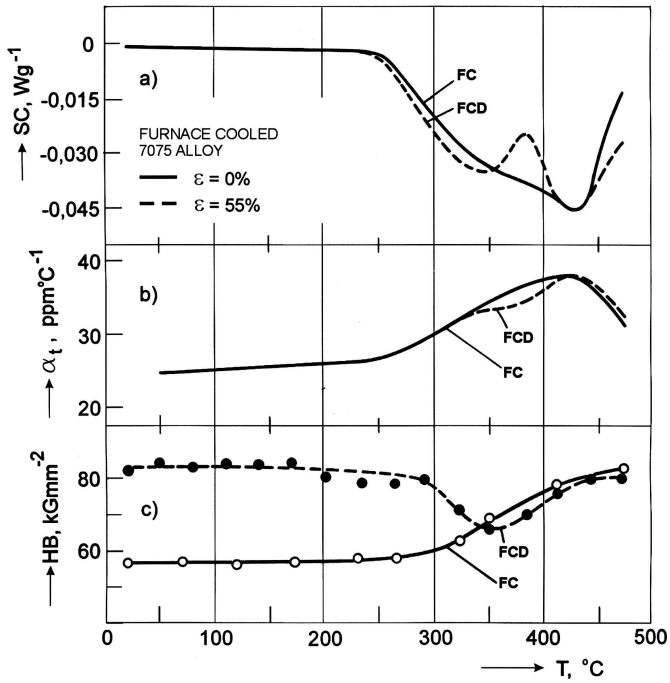

Fig. 1. Heating effects for as-furnace cooled (FC) AA7075 alloy and as-furnace cooled and deformed (FCD) AA7075 alloy, observed at constant heating rate of 15°C/min: a) calorimetric curve (DSC); b) dilatometric characteristics; c) Brinell hardness vs. annealing temperature curves

It can be confusing that the hardness of FC-samples raises with temperature above 250°C. The last effect is caused by the dissolution of η-particles which leads to solid solution hardening of the annealed material. On the other hand, initial hardness of FCD-samples was found to decrease in the temperature range 300-350°C that result mostly from advanced recovery as well by initiated recrystallization processes of alloy (Fig. 3b). Following increase of annealing temperature enhances solution hardening as mentioned formerly for FC-samples (Fig. 1c). Particles dissolution is also associated with detectable increase of the thermal expansion coefficient α_t, as shown in Fig. 1b for both FC and FCD samples. The maximum value of α_t (~ 38 ppm°C^{-1}) was observed at 425°C that corresponds to the endothermic peak in DSC curve.

3.2. Solution treated specimens

On the contrary to FC-type sample characteristics, both DSC and α_t vs. temperature curves for ST- and STD-samples reflect relatively complex precipitation sequences and following dissolution of particles including recrystallization of STD-material. It is commonly accepted that the first exothermic peak for solution treated AA7075 alloys, which is also observed at 95°C for ST-sample (Fig. 2a), result from Guinier-Preston zones development [2-4]. The peak is usually suppressed for solution treated and deformed (STD) alloy (Fig. 2a). The second peak on DSC curve, observed at ~240°C and

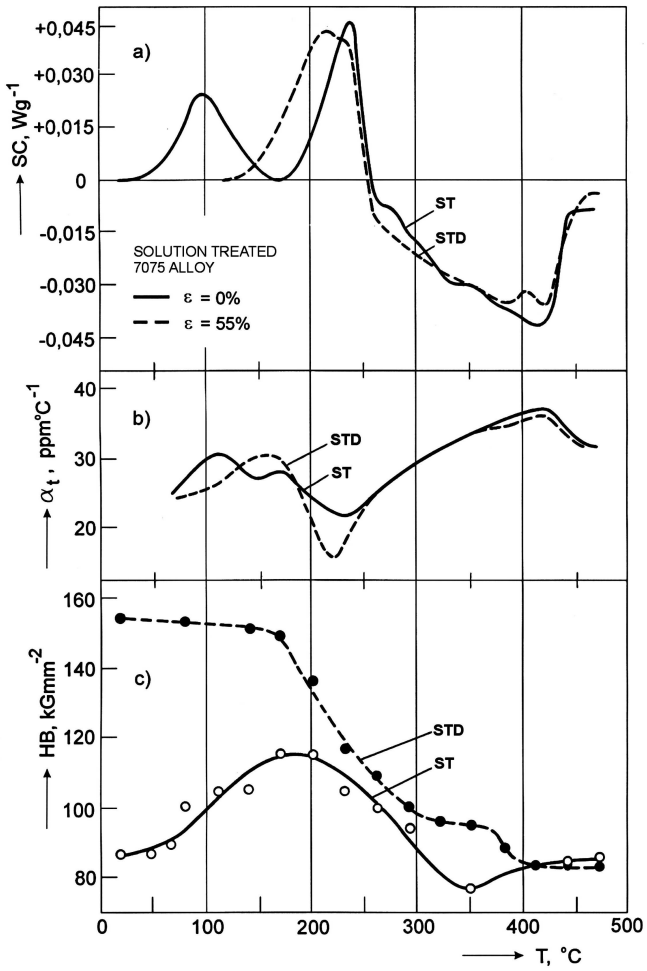

Fig. 2. Heating effects for as-solution treated (ST) AA7075 alloy and as-solution treated and deformed (STD) AA7075 alloy, observed at constant heating rate of 15°C/min: a) calorimetric curve (DSC); b) dilatometric characteristics; c) Brinell hardness vs. annealing temperature curves

~215°C for ST and STD samples, respectively, result from the precipitation of disperse η' and η particles [2, 3, 5, 6]. It seems reasonable to conclude that core diffusion in the presence of dense dislocation substructure as well as accelerated nucleation of fine particles on dislocation tangles caused the reduction of the peak's temperature for STD-samples. Development of the particles was confirmed by TEM observations and SAD pattern analysis as shown in Fig. 4a,b. Fine spots, observed between relatively strong aluminum spots in $< 11\bar{2} >$ diffraction pattern (Fig. 4b), are usually considered as an evidence

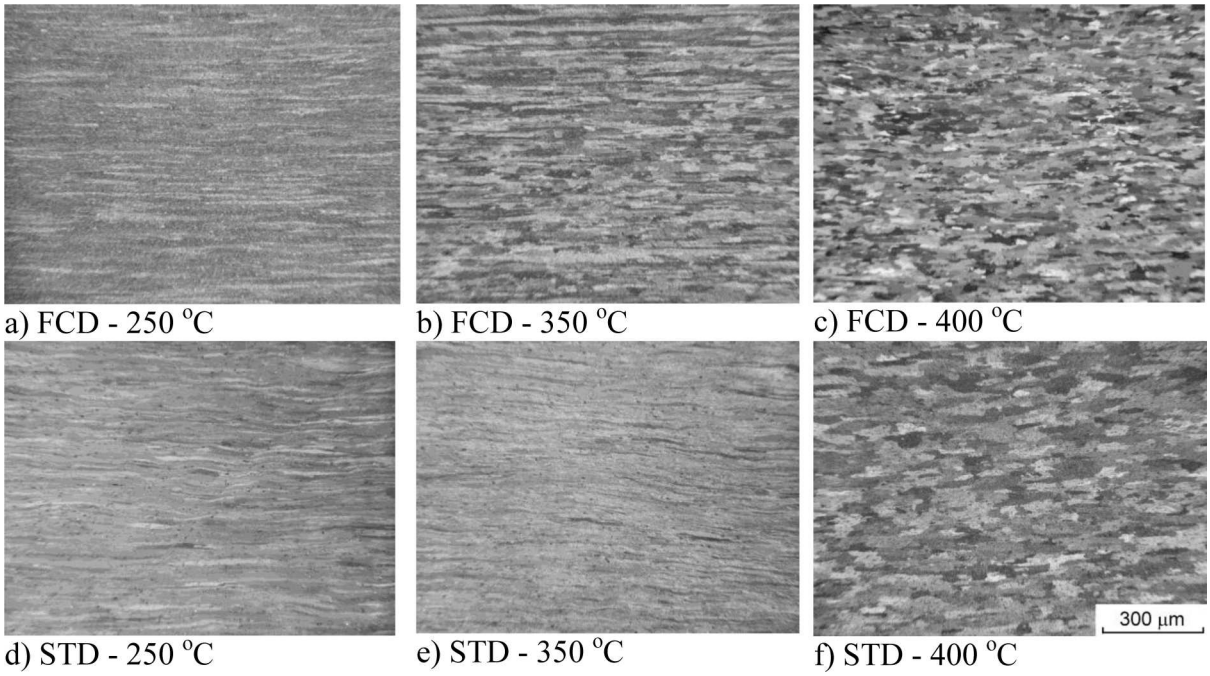

Fig. 3. Microstructure of AA7075 alloy in FCD and STD states after heating to the temperature: 250°C (a,d); 350°C (b,e) and 400°C (c,f). Heating rate 15°C/min

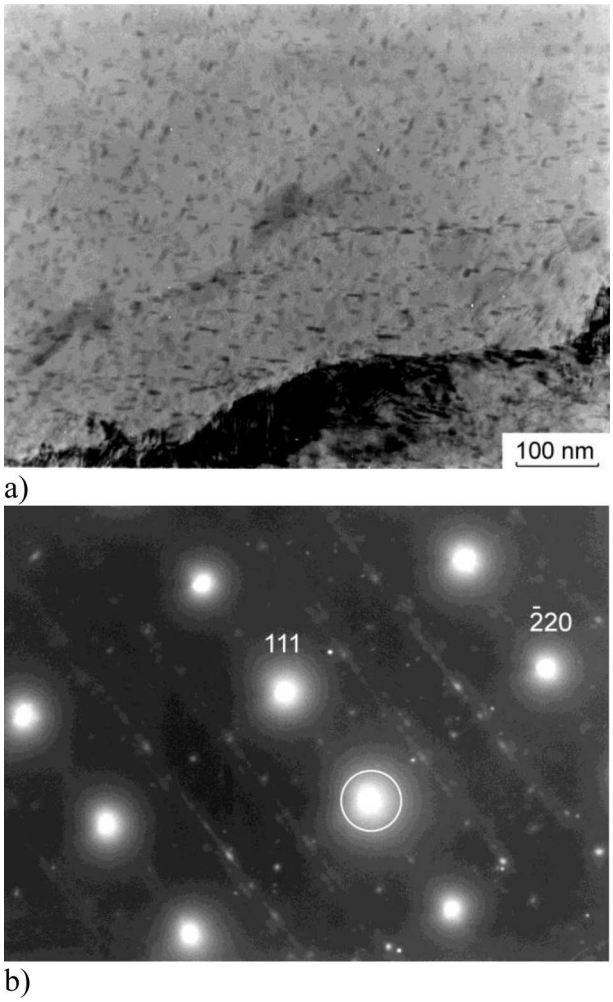

Fig. 4. Structure of as-solution treated (ST) AA7075 alloy heated at 15°C/min up to temperature 240°C (STEM) (a). Selected diffraction pattern $< 11\bar{2} >$ shows spots for η‘ i η that are observed between aluminum spots of <220> type (b)

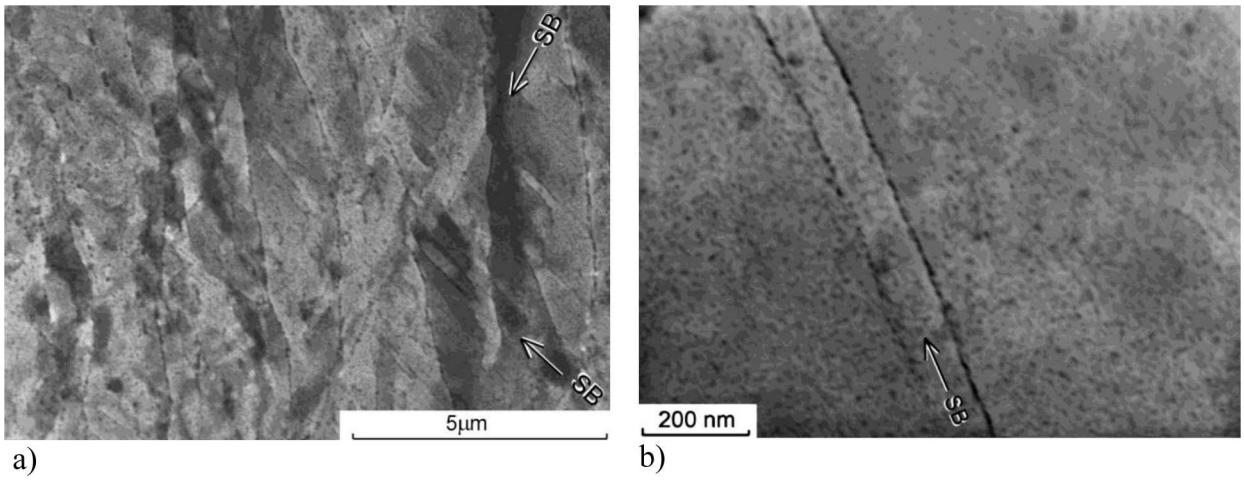

Fig. 5. Structure of as-solution treated and deformed (STD) AA7075 alloy, heated at 15°C/min up to temperature: a) 140°C (TEM); b) 240°C (STEM)

of mentioned phases development [2, 20]. Detection of fine η' or η particles with STEM, in the presence of dense dislocation tangles in STD sample, was difficult because of the low magnification and particle / dislocation contrast overlapping (Fig. 5). However, privileged nucleation and growth of the particles at subboundaries, grain boundaries and shear bands is evident. The last observations confirm previously mentioned reasons for the second peak temperature lowering at STD-samples.

Increasing temperature result in a wide endothermic peak on DSC curves having the minimum at ~425°C. The heat effect is related to the dissolution of particles that starts at ~250°C. Heat effects become very similar for both FC and FCD samples (Fig. 2a). Very fine exothermic peak at ~400°C can be ascribed to recrystallization of STD-samples (Fig. 3d-f). However, the heat flow is not as spontaneous as for FCD-samples and the maximum is shifted to higher temperature range, 380-420°C (Fig. 2a). As the grain boundary migration depends on the particles distribution, reduced recrystallization effect at STD samples may result from higher dispersion of the particles in STD-samples than those in FCD-material. Moreover, preliminary cold rolling of the solution treated material was found to result in shear bands development (Fig. 5a). Therefore, preferred nucleation of particles at the shear band edges as well as some other structural imperfections, contribute to the retardation of the recrystallization process. Enhanced coarsening of particles, which nucleate on shear band edges, is evident (Fig. 5b) and confirm similar effects presented in some previous papers [10-12, 19].

Variations of measured α_t value were found to follow similar sequences to these on DSC curves (Figs. 1b and 2b). The average α_t value depends on both pure thermal expansion of aluminum-matrix and over-imposed dilatometric effects induced by the phase transformation and related difference in the specific volume of structural components. First exothermic peak on DSC curve for ST-sample was found to result in increasing α_t value. It was assumed that increased elongation of sample could result from rising internal stresses in the matrix due to G-P zone development. Following nucleation and growth of η' and η particles causes reduction of the sample length (i. e. the increase of the material density). Higher reduction of α_t value for STD sample than that for ST suggests more intensive precipitation of η' and η particles. The last conclusion, as it seems, is consistent with high exothermic effect at 200-260°C as shown in Fig. 2a.

Dissolution of η particles at high annealing temperatures manifests itself by an extra elongation of the sample that overlap a thermal expansion at 250-425°C, as can be detected from α_τ vs. T characteristics shown in Figs. 1b and 2b. The last effect suggests that relatively high density of thermodynamically stable structure containing η particles in Al-matrix is decreased while η particles dissolve at high enough temperature. Total dissolution of η phase enriches the Al-matrix with ~2.5 at% Zn and ~2.6 at% Mg. Atomic radius of aluminum, 0.143 nm, is higher than that for Zn (0.133 nm), therefore, dissolution of Zn in Al-matrix can slightly increase of material density. However, dissolution of Mg lead to the predominated Al-matrix lattice expansion that is responsible for an extra elongation of the sample. The process of η phase dissolution become decayed above the temperature 425°C and the intensity of thermal elongation is reduced. As a result, further changes of density of the alloy at higher temperature range become returned to that resulting from typical thermal expansion of Al-matrix.

Hardness measurement results for ST-type specimens are shown in Fig. 2c. Maximum hardening effect was observed at 170-200°C, i.e. 30-70°C below the peak

on DSC curve that is ascribed to η' and η particles growth. Hardness maximum observed for ST-samples corresponds to the transformation of G-P zones into η' or at the most, some initial stage of η' $+\eta$ particles development. Following decrease of hardness for ST-samples heated to higher temperatures associates with the overageing process. The softening of STD-samples annealed at increasing temperature is caused by the overageing and the recovery processes. As the reduction of STD-material hardness starts at ~170°C without any detectable maximum on hardness vs. annealing temperature curve (Fig. 2c), it seems reasonable to conclude that the initial stage of softening predominates the overageing process. This conclusion is supported by accompanied effect of deep lowering of α_t value for FCD-samples (Fig. 1b). Mentioned above effects for both ST and STD samples suggest that commonly accepted maximum hardening at $\eta' \rightarrow \eta$ transformation range is not fully confirmed for non-isothermal annealing conditions. Maximum hardening of ST and STD material is related rather to G-P $+\eta$' development than usually accepted η' $+\eta$ precipitation effects.

TEM observations of samples heated to 465°C confirmed the dissolution of η particles independently to the preliminary heat treatment conditions. Remaining particles are enriched with copper and manganese that point to the development of undissolved θ-Al_2Cu and Al_6Mn phases (Fig. 6).

4. Conclusions

1. Thermal expansion coefficient (α_t) for solution treated AA7075 aluminum alloy was found to increase at 50-150°C during heating of the sample in accordance with an exothermic peak development on DSC curve. The peak, observed at ~100°C, is related to G-P zones development. Therefore, the effect of thermal expansion increase and following reduction of α_t were ascribed to competitive processes of G-P zones development, that induce the internal lattice stress development, and reduction of aluminum lattice parameters due to diffusion of alloying elements from Al-matrix to the growing particles.

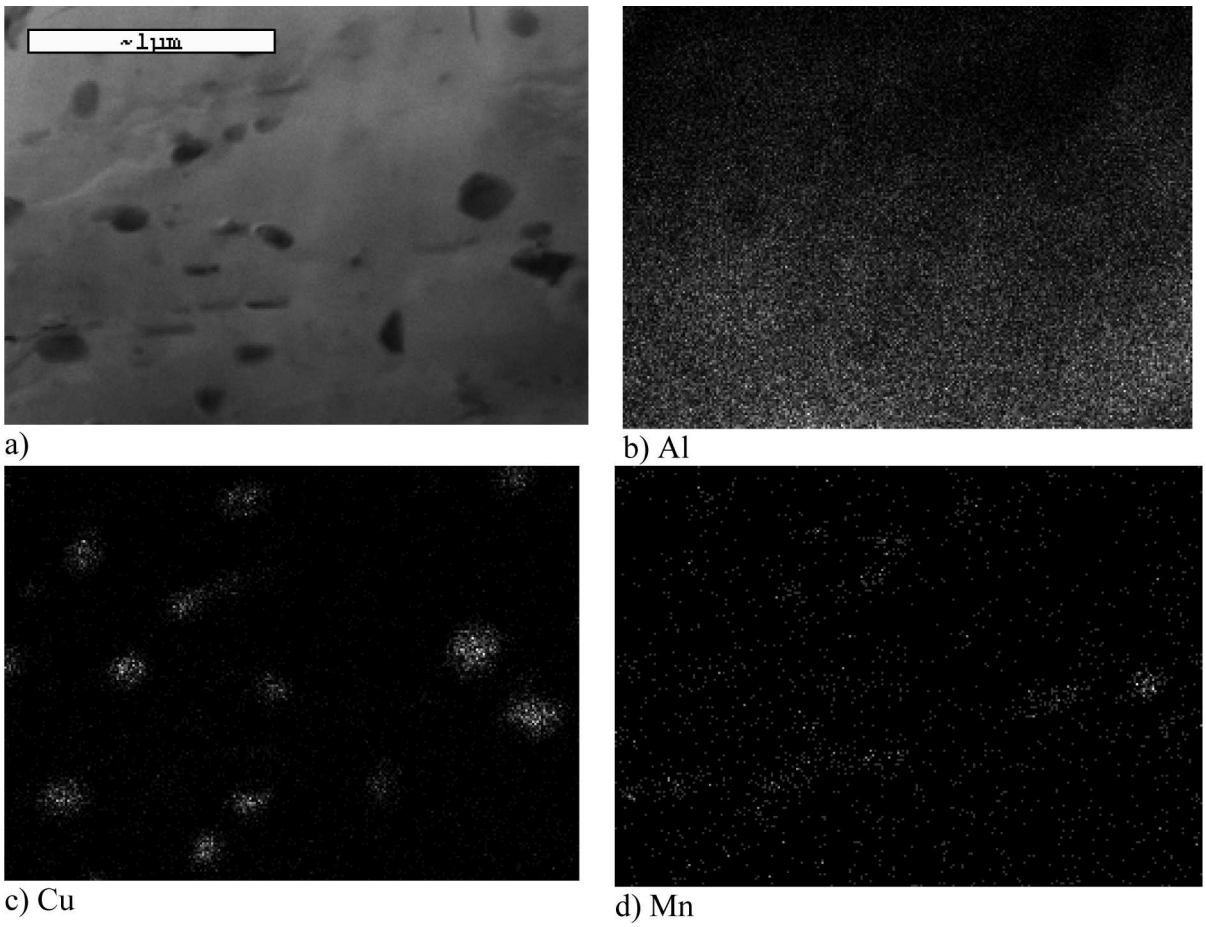

Fig. 6. Structure of preliminary furnace cooled (FC) AA7075 alloy, heated at 15°C/min up to temperature 465°C. STEM picture (a) and related mapping results for aluminum (b), copper (c) and manganese (d) elements

2. Deformation of preliminarily solution treated samples was found to result in decay of the peak for G-P zones. Following exothermic peak, ascribed to η' and η particles growth is shifted from 240°C to 215°C for solution treated sample (ST) and the sample deformed 55% (STD), respectively.

3. Increasing temperature affects the elongation coefficient α_t in accordance with the modification of the material structure. Nucleation of η', η particles is accompanied by the shrinking effect at 180-250°C, i.e. reduction of α_t value during continuous heating of ST-samples. Thermodynamically stable structure of slowly cooled FC-samples results in remaining of α_t at constant value up to ~250°C. Apart from the metallurgical state of tested alloy, following dissolution of constituent hardening phases, in particular η particles, starts at 250°C that was found to be accompanied by the increase the α_t value up to the maximum at 425°C.

4. Cold rolling of solution treated alloy increases the material hardness, from 87 HB to 155 HB for ST and STD samples, respectively. Following heating of solution treated samples results in the precipitation hardening of ST-material that raises the hardness value to the maximum 115HB after heating to 180-200°C. Effects of coarsening of precipitates (overageing) and recovery result in the reduction of the material hardness during annealing at 200-350°C.

5. Dissolution of η-particles and recrystallization overlap at high temperature annealing of STD and FCD samples. It is accompanied by widespread opposite heat effects, i.e. superimposing endothermic and exothermic effects related to the mentioned above structural processes. Therefore, the recrystallization peak is suppressed particularly at STD-samples. Recrystallization temperature of solution treated material (STD) was found to be approximately 25°C higher than that for furnace-cooled (FCD) material.

Acknowledgements

Financial support from the National Science Centre, under Grant No. UMO-2011/01/B/ST8/03012, is kindly acknowledged.

Received: 20 March 2012.

REFERENCES

[1] S. Yannacopoulos, S.O. Kasap, A. Heday-at, A. Verma, Canad. Met. Quart. **33**, 51 (1994).
[2] E. Salamci, Mat. Sci. Techn. **20**, 859 (2004).
[3] D.J. Lloyd, M.C. Chaturvedi, J. Mater. Sci. **17**, 1819 (1982).
[4] C. Garcia-Cordovilla, E. Louis, Mat. Sci. Eng. **A132**, 135 (1991).
[5] R. DeIasi, P.N. Adler, Met. Trans. **8A**, 1177 (1977).
[6] A. Deschamps, Y. Bréchet, F. Livet, Mat. Sci. Techn. **15**, 993 (1999).
[7] X. Li, M.J. Starink, Mater. Sci. Forum, **331-337**, 1071 (2000).
[8] A. Deschamps, F. Livet, P. Guyot, Y. Bréchet, Z. Metallkunde **88**, 601 (1997).
[9] A. Deschamps, F. Livet, Y. Bréchet, Acta Mater. **47**, 281 (1999).
[10] K. Pieła, A. Korbel, Mat. Sci. Forum **217-222**, 1037 (1996).
[11] A. Korbel, W. Bochniak, F. Ciura, H. Dybiec, K. Pieła, Proc. TMS Annual Meeting, Orlando (USA), 301 (1997).
[12] A. Korbel, W. Bochniak, F. Ciura, H. Dybiec, K. Pieła, J. Mater. Proc. Techn. **78**, 104 (1998).
[13] L.F. Mondolfo, Aluminum Alloys: Structure and Properties. Butterworths & Co. (Publ.) Ltd., p. 577 London 1976.
[14] L.M. Clarebrough, M.E. Hargreaves, G.W. West, Phil. Mag. **1**, 528 (1956).
[15] L.M. Clarebrough, M.E. Hargreaves, G.W. West, Acta Met. **5**, 738 (1957).
[16] L.M. Clarebrough, M.E. Hargreaves, M.H. Loretto, G.W. West, Acta Met. **8**, 797 (1960).
[17] S. Nebti, D. Hamana, G. Cizeron, Acta Met. Mat. **43**, 3583 (1995).
[18] L. Katgerma, D. Eskin, in: Handbook of Aluminum, Ed. M. Dekker, Inc., vol. **1**, p. 259 New York – Basel 2003.
[19] L. Błaż, K. Pieła, Mat. Sci. Techn. **23**, 400 (2007).
[20] J.M. Papazian, Met. Trans. **13A**, 761 (1982).